Azerbaijan University of Architecture and Construction
ISSN 2706-7726
Engineering Mechanics
Scientific and Technical Journal
E-mail: engineeringmechanics@azmiu.edu.az

September 2025	Issue 21	Volume 13	Number 3	Pages 14-20

SEISMIC RESPONSE ASSESSMENT AND ISOLATOR DESIGN FOR A LONG-SPAN CABLE-STAYED BRIDGE

Ramiz ISKANDEROV[1], Sevket ATES[2], Nijat MASTANZADE[3], Tural RUSTAMLI[4], Nariman ABDINLI[5]

[1]*Azerbaijan University of Architecture and Construction*, r.iskanderov@gmail.com , *Baku, Azerbaijan,*
[2]*Karadeniz Technical University, Department of Civil Engineering, 61080* sates@ktu.edu.tr *Trabzon, Turkey*
[3]*Azerbaijan Technical University, nijat.mastanzadeh@aztu.edu.az , Baku, Azerbaijan*
[4]*Hydrotrans Engineering Ltd. rustamli.tural.90@gmail.com, Baku, Azerbaijan*
[5]*Sumgayit Technology Park, n.abdinli@outlook.com, Baku, Azerbaijan*

Abstract: This paper presents a comprehensive dynamic investigation of Azerbaijan's longest planned cable-stayed bridge—a multi-span structure with a 1,100 [m] main span—subjected to dead, live (A-15), and seismic (MSK-64 IX) loads. Using detailed finite-element models in SAP2000, we quantify how cable pretension influences the global stiffness, modal periods, and internal force distribution. A single-concave friction pendulum (SCFP) isolation system (R = 6 [m], μ = 0.08) is iteratively designed to achieve an effective isolator stiffness of 3,415 [kN/m], a fundamental period extension from 2.0 [s] to 4.2 [s], and a displacement capacity of 0.78 [m]. Spectral acceleration demands drop by up to 40%, translating into 20–30% reductions in deck shear forces and cable tension peaks. The results demonstrate that SCFP bearings significantly enhance seismic resilience for long-span cable-stayed bridges in high-activity regions.

Keywords: *Seismic isolation, Cable-stayed bridges, Finite element model, Single concave friction pendulum (SCFP) bearing*

INTRODUCTION

Large-span cable-stayed bridges are increasingly dominating the bridge infrastructure. These structures consist of one or more pylons connected to the roadbed by means of steel ropes—cables [1-5]. The pylons, in turn, are not connected to the bridge supports. For example, this work examines the project of the largest multi-span cable-stayed bridge in Azerbaijan, currently under construction on the Muganly-Ismayilli-Gabala road [6]. This bridge has a total length of 1100 [m] (Fig. 1). According to Azerbaijan's seismic zoning map, the Muganly-Ismayilli-Gabala road lies within an active seismic zone. Based on the international seismic scale, earthquakes in this region may reach an intensity of 9_2 on the MSK-64 scale, with such an event potentially occurring once every 100 years [5]. An earthquake intensity index of 2 indicates low seismic activity. If the seismic score of the bridge site is calculated as $I_u = 9$, an earthquake of this magnitude could be expected to occur up to

once in a 100-year period. Considering that the construction site of the bridge is located in a region of high seismic activity, the issue of dynamic stability is highly relevant. To reduce the response to seismic shocks, kinematic roller supports are provided between the bridge's stiffening beam and the supports. The A-15 live load has been selected, representing a vehicle load with an axial force of 15 [kN], applied to the bridge in accordance with regulatory guidelines.

Figure 1. General view of the bridge

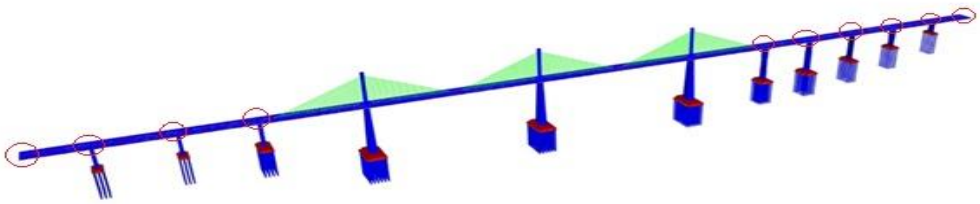

Figure 2. Computational model of the bridge by CSI Bridge program

MODELLING OF BRIDGE. ACTUAL LOADS

Bridge modeling was carried out on the SAP2000 computer program. Points marked with a red circle are places where seismic isolators (Figure 2). The isolators are installed at the marked locations, and in the dynamic equation, the term F_{eff} on the right-hand side represents the seismic force. This includes β the dynamic coefficient. Here, the acting seismic force is determined by the impact of the mass, which is an obstacle, into the impulse of soil occurrence: $F_{eff} = m\ddot{x}_g$. In addition to the seismic force, the bridge is affected by various loads. Their combination according to the norms is taken in the form of the following formula:

1.0 Loads + 0.5 Availability + 0.5 Available load + 0.8 seismic load (1)

Superstructures of extradosed bridges are an intermediate type between continuous beam and warp bridges. Cables in extra bridges provide preliminary stressed stiffening beams and take up vertical load. Seismic isolators used on bridges vary in design, with their primary goal being to consistently reduce the maximum vertical load exerted by the bridge beams. On large-scale structures, kinematic spherical movable supports are employed. These supports are named as single concave friction pendulum bearings (SCFP) (Fig. 3). The fundamental principle of these supports is to mitigate the

vertical load on the supports by allowing the spherical or cylindrical component within the hemispherical support to shift in response to horizontal seismic forces. Bearings are located in a closed metal box. The layout of the seismic isolator (SCFP) between the pylon and the stiffening beam is shown in Figure 4.

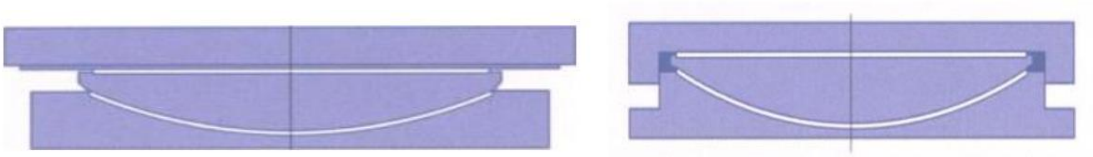

Figure 3. Fixed and moving friction pendulum bearing supports

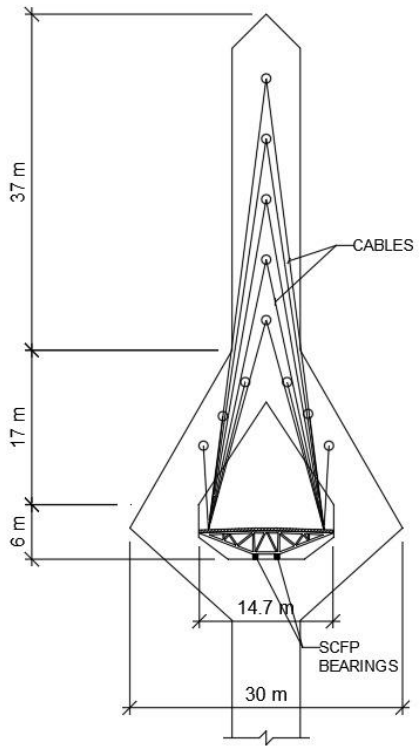

Figure 4. Cross section of the bridge section and layout of the seismic isolator between the pylon and the stiffening beam

DYNAMIC ANALYS OF THE BRIDGE

The dynamic equation of bridge is

$$M\ddot{u} + C\dot{u} + Ku = F_{eff} \tag{2}$$

Where $\ddot{u}$, $\dot{u}$, u are respectively acceleration, velocity and displacement of the bridge's elements – cables and stiffness beam. The stiffness consists of cable stiffness and girder stiffness:

$$K_c = \frac{A_c E_{eq}}{l_0}\begin{bmatrix} 1 & 0 & -1 & 0 \\ 0 & 0 & 0 & 0 \\ -1 & 0 & 1 & 0 \\ 0 & 0 & 0 & 0 \end{bmatrix} \tag{3}$$

Where A_c is a cross section of the cable; l_0 is a length of cable; E_{eq} is a equivalent elastic modulus of the cable, which definition as

$$E_{eq} = \frac{E}{1+\frac{\gamma^2 l_0}{12\sigma^2}} \tag{4}$$

And girder stiffness

$$K_b = \begin{bmatrix} \frac{AE}{l}S_5 & 0 & 0 & -\frac{AE}{l}S_5 & 0 & 0 \\ 0 & \frac{12E}{l^3}S_1 & \frac{GEI}{l^2}S_2 & 0 & -\frac{12EI}{l^3}S_1 & \frac{6EI}{l^2}S_2 \\ 0 & \frac{6EI}{l^2}S_2 & \frac{4EI}{l}S_3 & 0 & -\frac{6EI}{l^2}S_2 & \frac{2EI}{l}S_4 \\ -\frac{AE}{l}S_5 & 0 & 0 & -\frac{AE}{l}S_5 & 0 & 0 \\ 0 & \frac{12E}{l^3}S_1 & \frac{GEI}{l^2}S_2 & 0 & \frac{12EI}{l^3}S_1 & -\frac{6EI}{l^2}S_2 \\ 0 & \frac{6EI}{l^2}S_2 & \frac{2EI}{l}S_4 & 0 & \frac{6EI}{l^2}S_2 & \frac{4EI}{l}S_3 \end{bmatrix} \tag{5}$$

Where $S_1 = (\gamma l)^3 \frac{\sin(\gamma l)}{12R_c}$; $S_2 = (\gamma l)^2 \frac{[1-\cos(\gamma l)]}{6R_c}$; $S_3 = (\gamma l) \frac{[\sin(\gamma l)-(\gamma l)\cos(\gamma l)]}{4R_c}$; $S_4 = (\gamma l) \frac{[\gamma l-\sin(\gamma l)]}{2R_c}$; $S_5 = \frac{1}{\left[\frac{1+(EAR_{cm})}{4P^3 l^2}\right]}$. In this $\gamma = \sqrt{\frac{P}{EI}}$; $R_c = 2 - 2\cosh(\gamma l) - (\gamma l)\sinh(\gamma l)$; $\boldsymbol{G}$ is the shear modulus; $\boldsymbol{I}$ is the moment of inertia.

$$R_{cm} = (\gamma l)(M_{ab}^2 - M_{ba}^2)[\coth(\gamma l) + (\gamma l)\,\mathrm{csch}(\gamma l)^2] - 2(M_{ab} + M_{ba})^2$$
$$+(M_{ab} \times M_{ba})[1 + (\gamma l)\,\mathrm{csch}(\gamma l)][2(\gamma l)\,\mathrm{csch}(\gamma l)] \tag{6}$$

Cable stiffness is calculated based on elastic stiffness $\boldsymbol{K_E}$ and geometric stiffness $\boldsymbol{K_g}$. The reduction in load on the cables caused by each stress results in their inclination, which subsequently induces vibrations in the structure.

$$K_i = K_E + K_g = \frac{EA_i}{l_0}\begin{bmatrix} \cos^2\theta & \cos\theta\sin\theta \\ \cos\theta\sin\theta & \sin^2\theta \end{bmatrix} + \frac{N}{L}\begin{bmatrix} 1 & 0 \\ 0 & 1 \end{bmatrix} \tag{7}$$

Where $\boldsymbol{E}$ is the modulus of elasticity of the cable material; A_i is the cross sectional area of the $\boldsymbol{i}$-cable element; l_0 is a length of unstressed cable; *cos* θ, *sin* θ are angular function of cable stiffness to the horizontal region; N is the longitudinal tension;

Analogy may to write for mass matrix. Matrix mass of beam will be:

$$m_b = \frac{m_{bc}}{420}\begin{bmatrix} 140 & 0 & 0 & 70 & 0 & 0 \\ 0 & 156 & 221 & 0 & 54 & -13l \\ 0 & 22l & 4l^2 & 0 & 13l & -3l^2 \\ 70 & 0 & 0 & 140 & 0 & 0 \\ 0 & 54 & 13 & 0 & 156 & -22l \\ 0 & -13l & -3l^2 & 0 & -22l & 4l^2 \end{bmatrix} \tag{8}$$

And matrix of cable

$$m_c = \frac{n_c}{6}\begin{bmatrix} 2 & 0 & 1 & 0 \\ 0 & 2 & 0 & 1 \\ 1 & 0 & 2 & 0 \\ 0 & 1 & 0 & 2 \end{bmatrix} \tag{9}$$

The damping matrix is function stiffness and mass matrices of the bridge as

$$[C] = \alpha[M] + \beta[K] \tag{10}$$

Where $\boldsymbol{\alpha}$ and $\boldsymbol{\beta}$ are the Rayleigh damping factors, which can be investigated by having two structural damping ratios $\boldsymbol{\xi}$ associated with two specific frequencies.

ISOLATOR SYSTEM CALCULATION

The choice of isolator is designed for vertical load (bridge weight and moving loads). The total average isolatorr load was taken as 15000 [kN]. Preliminary accepted radius R = 6 [m], friction coefficient 0.08. At the conclusion of the iterative calculation, the effective stiffness of a single isolator was determined to be 3415 [kN/m]. From this calculation, the displacement capacity of a single isolator was found to be approximately 0.78 [m]; accordingly, a single-concave friction pendulum bearing with an 0.80 [m] displacement capacity, a 15 000 [kN] vertical load rating, and a 6 [m] curvature radius was selected from the manufacturer's catalogue for use in the finite-element model. The number of isolators was determined to be 20. Calculations were carried out in PYTHON and SAP2000 computer program. The results of calculations for selection of seismic isolators are presented on graphs and in tabular form by using nominal parameters of the isolators. Calculations were carried out in accordance with the Turkish Earthquake Code [4]. Through successive iterations, the bridge's fundamental vibration period was refined to 4.2 [s]

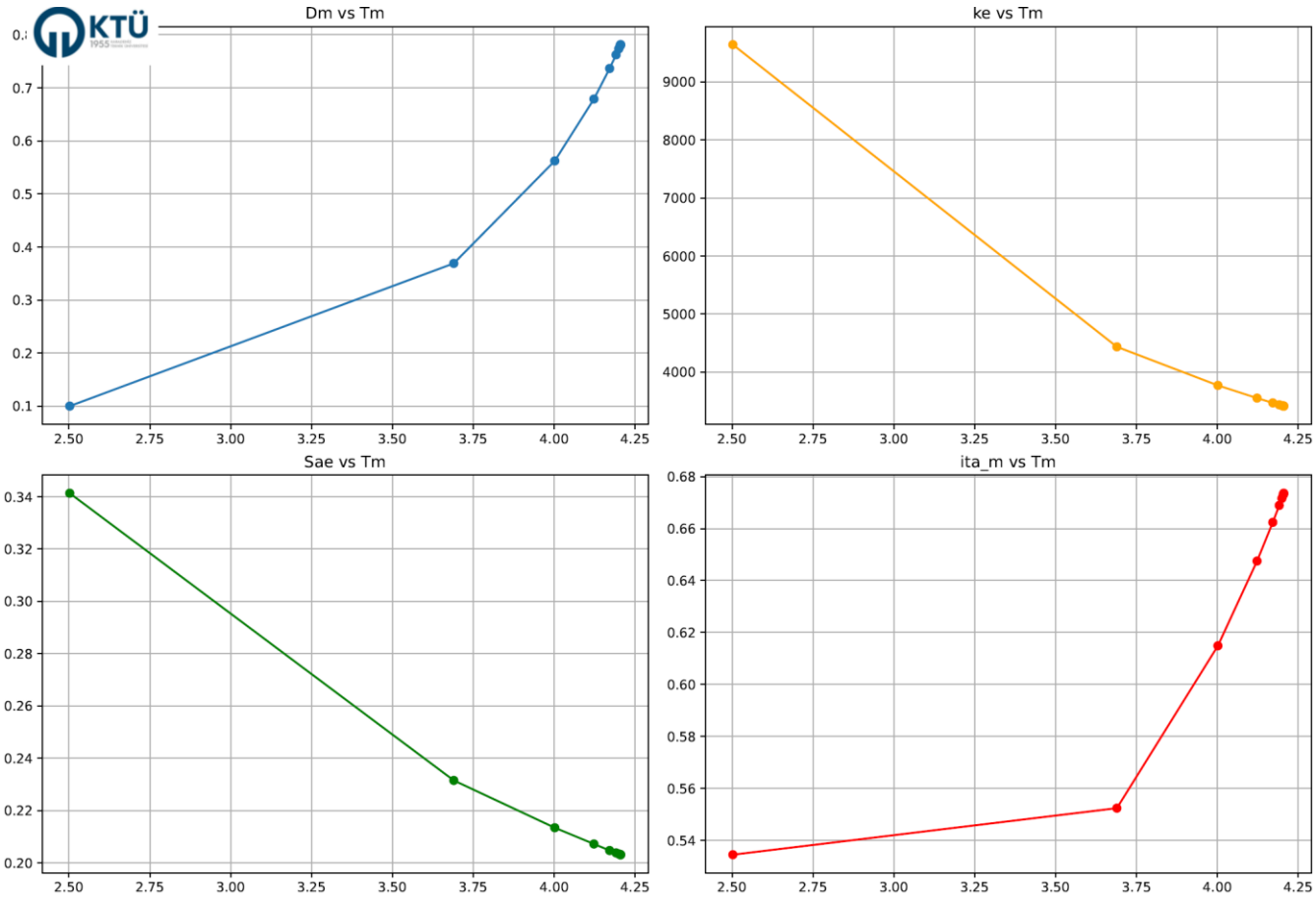

Figure 3. Plot of relationship between oscillation period and isolator diameter

In this study, S_{ae} is a horizontal spectral acceleration, S_{DS} is a short period spectral acceleration coefficient, S_{D1} is a spectral acceleration factor calculated for a period of 1.0 [s].

Table 1. Iterative SCFP Isolator Calculation Results

Diameter D_m ***[m]***	K_e ***[kN/m]***	β	ξ ***eff (%)***	η	T_m ***[s]***	S_{ae} ***(g)***
0.1000	9640	0.4715	30.0000	0.5345	2.5024	0.3413
0.369	4435	0.2778	27.7754	0.5524	3.6893	0.2315
0.5622	3770	0.2145	21.4462	0.6149	4.0015	0.2134
0.6788	3552	0.1885	18.8529	0.6475	4.1225	0.2072
0.7364	3470	0.1779	17.7907	0.6624	4.1711	0.2047
0.7622	3437	0.1735	17.352	0.6689	4.191	0.2038
0.7733	3423	0.1717	17.1699	0.6716	4.1992	0.2034
0.7780	3418	0.1709	17.0941	0.6728	4.2027	0.2032
0.7800	**3415**	**0.1706**	**17.0625**	**0.6732**	**4.2041**	**0.2031**

CONCLUSION

In this study, a detailed dynamic analysis of an 1100 [m] multi-span cable-stayed bridge demonstrated that single concave friction pendulum (SCFP) bearings effectively reduce seismic demands on the deck and pylons. The influence of cable tension on global stiffness and the selection of isolator geometry and friction properties was validated through SAP2000, and Python-based calculations.

1) The weight of the cargo bridge, the floor, the weight of the cable, is taken as a constant load. AK-15 types of automobile cargo are accepted as temporary cargo. It is a load falling from the car's four-lane wheels.

2) Cable quality, tensile strength, cross section and specified stress have a strong influence on the overall dynamic stiffness and durability of cables.

3) The dynamic stability of cable bridges is influenced by the tension force of cables. Therefore, it is necessary to check the strength, durability of cables and rigidity of the bridge beams. The Ismailli Bridge project, considered an analog bridge, meets these conditions.

4) The results show that usage of isolation devices offers some advantages for the internal forces on the deck for the considered isolated bridge as per the non-isolated bridge. Finally, it should be noted that isolation system is more effective when the bridges are subjected to earthquakes. The current modelling approach assumes linear elastic behavior for cables and girders, Rayleigh damping, and neglects soil-structure interaction and geometric nonlinearities at large displacements. Additionally,

the isolator performance is evaluated under one-directional seismic inputs without accounting for multi-axial excitations, temperature effects, aging, or degradation over the service life. Future research could address these limitations and further optimize the design by: implementing nonlinear time-history analyses under multi-directional ground motions to capture realistic isolator hysteresis and energy dissipation. Incorporating soil-structure interaction to assess foundation flexibility and its impact on global seismic response. Performing parametric optimization of isolator radius, friction coefficient, and damping characteristics using automated Python routines.

Extending the model to include aerodynamic loads, temperature variations, and long-term aging effects on bearing performance. Validating numerical predictions with scaled laboratory testing or ambient vibration monitoring on an as-built bridge.

REFERENCES

1. AzDTN 2.1-1. Loads and influence. Baku.2015.
2. AzDTN 2.05.03.84. Bridge and pipes. Bakı.2011.
3. AASHTO LRFD. Bridge Design Specification. 8th Ed.Sept.2017.
4. Disaster and Emergency Management Presidency (AFAD), "Turkish Building Seismic Code (TBEC-2018)," Official Gazette, no. 30316, Mar. 18, 2018.
5. F. Yang, H. Zhao, A.L, Z. Fang. Experimental-numerical analysis on the cable vibration behavior of a long-span rail-cum-road cable-stayed bridge under the action of high-speed trains, Applied Science.2023,13,11082.
6. Papadopolus P.G., J. Arethas, P. Lazaridis. Numerical study on the behavior of cables of cable-stayed bridges. Earthquake Resistant Engineering. WIT Transaction on the Built Environment, Vol.81. 2005.
7. Muganli-Ismayilli-Gabala road reorganization. Bridge over Aksu river. Design Project. Euroscon. Baku.202.
8. T.X. Ngueyen, D.V.Tran. A finite element model of vehicle – cable stayed bridge interaction considering braking and acceleration. The 2014 World Congress on Advances in Civil, Environmental and Materials Research (ACEM14) Busan, Korea, August 24-28, 2014.
9. Shrestha. Karnali cable-stayed bridge: Development of finite element model and free vibration analysis. J. of the Institute of Engineering. Vol. 10, No. 1, pp. 14-24.
10. C.Tie, Z.Ruichuan. Mechanical analysis of stayed bridge. The Open Mechanical Engineering Journal, 2015, 9, 780-785.
11. H.Naderian, M.M.S.Cheng, Z.Shei, E.Dragomirrescu. Seismic analysis of long-span cable-stayed bridges by an integrated finite strip method. J. Bridge Ebg. 2016, 21 (3) 04015068.
12. B.Atmaca, M.Yurdakul, Ş.Ateş. Nonlinear dynamic analysis of bridge isolated cable-stayed bridge under earthquake excitations. Soil Dynamics and Earthquake Engineering. 66 (2014) 314-318.